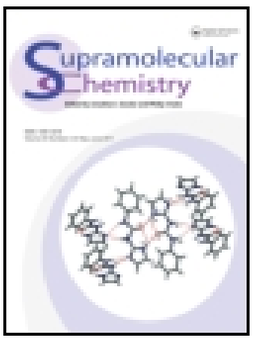

Supramolecular Chemistry

ISSN: (Print) (Online) Journal homepage: https://www.tandfonline.com/loi/gsch20

Adamantane appended antimicrobial supramolecular self-associating amphiphiles

Andzelika Rutkauskaite, Lisa J. White, Jessica E. Boles, Kira L. F. Hilton, Melanie Clifford, Bethany Patenall, Bree R. Streather, Daniel P. Mulvihill, Samantha A. Henry, Mark Shepherd, J. Mark Sutton, Charlotte K. Hind & Jennifer R. Hiscock

To cite this article: Andzelika Rutkauskaite, Lisa J. White, Jessica E. Boles, Kira L. F. Hilton, Melanie Clifford, Bethany Patenall, Bree R. Streather, Daniel P. Mulvihill, Samantha A. Henry, Mark Shepherd, J. Mark Sutton, Charlotte K. Hind & Jennifer R. Hiscock (2023): Adamantane appended antimicrobial supramolecular self-associating amphiphiles, Supramolecular Chemistry, DOI: 10.1080/10610278.2022.2161902

To link to this article: https://doi.org/10.1080/10610278.2022.2161902

Published online: 10 Jan 2023.

SUPRAMOLECULAR CHEMISTRY
https://doi.org/10.1080/10610278.2022.2161902

Taylor & Francis
Taylor & Francis Group

Adamantane appended antimicrobial supramolecular self-associating amphiphiles

Andzelika Rutkauskaite[a], Lisa J. White[a], Jessica E. Boles[a], Kira L. F. Hilton[a], Melanie Clifford[b], Bethany Patenall[b], Bree R. Streather[a,c], Daniel P. Mulvihill[c], Samantha A. Henry[c], Mark Shepherd[c], J. Mark Sutton[b], Charlotte K. Hind[b] and Jennifer R. Hiscock[a]

[a]School of Chemistry and Forensic Science, University of Kent, Kent; [b]National Infection Service, UK Health Security Agency (UKHSA), Porton Down, Salisbury SP4 0JG, UK; [c]School of Biosciences, University of Kent, Kent, CT2 7NH, UK

ABSTRACT

Herein, we present the synthesis of two novel adamantane appended supramolecular self-associating amphiphiles. The antimicrobial efficacy of these compounds is determined against both clinically relevant Gram-positive methicillin-resistant *Staphylococcus aureus* and Gram-negative *Escherichia coli*. We also explore the self-associative properties of these amphiphiles in both polar organic DMSO-d_6 0.5% H_2O and H_2O (D_2O)/EtOH 19:1 solutions, confirming aggregate stability through the determination of zeta potential values, aggregate size through a combination of ^{1}H NMR DOSY and dynamic light scattering studies as appropriate, and critical aggregate concentration through the derivation of concentration-dependent surface tension values. We also perform a variety of ^{1}H NMR dilution studies and in-silico modelling to further explore the roles of intermolecular hydrogen bonding and lipophilicity within aggregate formation and antimicrobial efficacy. Finally, we perform haemolysis and *Galleria mellonella* toxicity assays to establish the potential of these compounds to undergo further development as antibiotic agents.

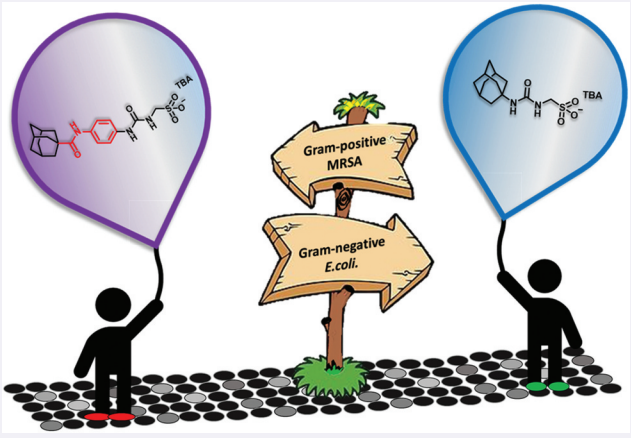

ARTICLE HISTORY
Received 1 August 2022
Accepted 19 December 2022

KEYWORDS
Hydrogen bond; antimicrobial; self-association; amphiphile

Introduction

One of the greatest threats to the global economy and public health is the rise of antimicrobial-resistant (AMR) bacterial infections. In 2019, the primary effects of AMR were found to be responsible for ≈ 3.57 million deaths worldwide, making it the third leading cause of global mortality [1]. A report commissioned by the UK government has predicted that this number will rise significantly by the year 2050, where an estimated 10 million deaths per year will be attributed to AMR alone [2], resulting in an annual one trillion dollar decrease in the global gross domestic product [3]. The cause of this continued rise in AMR-related deaths is considered to be due to multiple factors, which include the misuse of antibiotics/antimicrobials and antiseptics in both the veterinarian [4] and clinical [5,6] sectors, as well as failure to complete prescribed medicinal courses as advised by physicians [7]. In addition, the SARS-CoV-2 (Covid-19) pandemic has also contributed to the rise of AMR [8–10]; even though the spread of infection was limited due to restricted mobility [8], there has been a substantial increase in use of antibiotic agents worldwide [10] Most

CONTACT Jennifer R. Hiscock J.R.Hiscock@Kent.ac.uk School of Chemistry and Forensic Science, University of Kent, Canterbury, Kent

commonly administered amongst those who already have a compromised immune system 11, or are hospitalised, where ≈72% of patients were treated with antibiotics even though only 8% showed evidence of infection [11] Thus, there is a crucial need for the development of new antimicrobial agents in order to help combat the rise of AMR, the 'silent' global pandemic [10].

To date, the field of supramolecular chemistry has provided a variety of small molecular approaches to the development of novel antimicrobial agents. Examples of which include work by Cai and co-workers who investigated the therapeutic potential of a series of small-molecular-weight host-defence peptide mimicking antibiotic agents. These agents showed antimicrobial activity against clinically relevant multi-drug-resistant bacterial pathogens which included Gram-positive methicillin-resistant *S. aureus* (MRSA) and Gram-negative *Escherichia coli*. (*E. Coli*), with minimum inhibition concentration (MIC) values of between 0.16–1.56 μg/mL and 0.75–3.12 μg/mL, respectively [12]. In addition, Haldar and co-workers reported a new class of small antimicrobial molecule (SAM), incorporating aliphatic chains, quaternary ammonium, and ethanol functionalities with a design principle focusing on a hydrophobic and hydrophilic balance. These SAMs displayed low toxicity with a haemolytic concentration of 577 μg/mL required to lyse 50% of human erythrocytes. Furthermore, SAMs also demonstrated antimicrobial activity (MIC = 1–4 μg/mL) against clinical isolates of MRSA and vancomycin-resistant *S. aureus* (VRSA) [13]. Finally, Al-Tel and co-workers investigated the antimicrobial efficacy and selectivity of 29 cationic polyheterocyclic compounds, with 17 displaying activity against Gram-positive MRSA, *Bacillus subtilis and Enterococcus faecalis* with MIC values ranging 3.1–12.5 μg/mL [14].

Our own efforts in this area have focused on the development of a novel class of >70 supramolecular self-associating amphiphilic salts (SSAs) [15–21], the anionic component of which contains two principle hydrogen bond acceptor (HBA) sites and a single hydrogen bond donating (HBD) site, meaning these units self-associate in a 'frustrated' manor, as not all of the possible hydrogen bonding modes can be fulfilled simultaneously [22]. To date, SSAs have been shown to: selectively coordinate to phospholipid membranes of differing headgroup composition [23,24]; act as cisplatin enhancement agents against ovarian cancer cells [25]; enhance the activity of antimicrobial agents against clinically relevant microbes and ESKAPE pathogens [25–27]; have potential to act as drug delivery vehicles [19,20]; and finally, to act as antimicrobial agents against clinically relevant Gram-positive MRSA and Gram-negative *E. coli* [19,28,29].

It is hypothesised that the mode of action for this class of compounds is related to their inherent ability to selectively interact with and permeate phospholipid membranes of differing composition [28]. To enable us to explore how simple structural modifications to our generic SSA structure [30],[28] increasing lipophilicity, affects the physicochemical properties and resultant antimicrobial activity of our systems, we introduce compounds **1** and **3** (Figure 1). These molecules were designed to allow us to explore the effects of the adamantane functionality within the SSA structure, as this functionality is known to increase molecular biological membrane permeation properties, through increased lipophilicity. In addition, this functionality is also used to ensure molecular stability, improving molecular pharmacokinetic properties, which is an important consideration for novel therapeutic agents [30,31].

Pioneering early work saw the adamantane moiety incorporated into effective anti-influenza drugs against Influenza A in particular [32–35]. In addition, therapeutics incorporating the adamantane moiety have been used to combat immunodeficient viral infections such as HIV [36–39] and Hepatitis C [40], as well as in the development of anti-malarials [41,42], anti-inflammatories [43–45] and antimicrobials [46–48]. Specific examples relating to the use of this functionality within the structure of antimicrobial agents include work by Kadi and co-workers, who developed a novel series of 2-(1-adamantyl)-5-substituted-1,3,4-oxadiazoles and 2-(1- adamantylamino)-5-substituted-1,3,4-thiadiazoles.

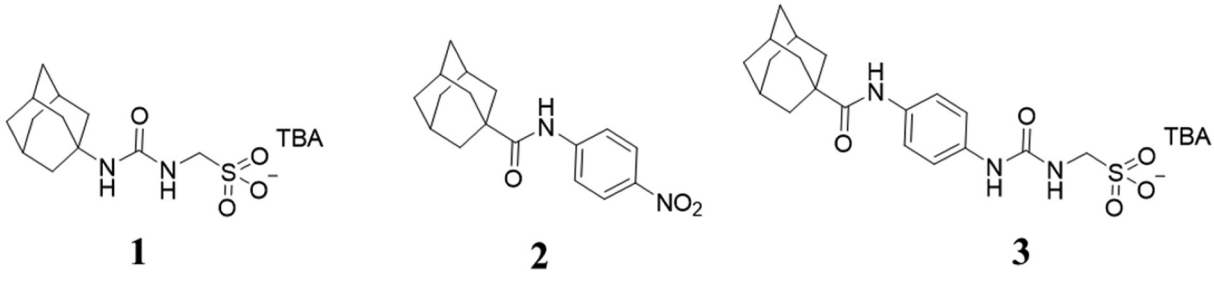

Figure 1. Chemical structures of SSAs **1** and **3**, and intermediate **2.**

The results of antimicrobial efficacy studies showed selectivity towards Gram-positive *Bacillus subtilis* IFO 3007 over *S. aureus* IFO 3060 and Gram-negative *E. coli* 3301 [44]. In addition, Orzeszko and co-workers established the antimicrobial efficacy for a series of 14 adamantane derivatives against a range of clinically relevant bacteria. Of these 14 compounds, 12 displayed activity towards Gram-positive *cocci* strains with MIC_{50} values ranging 0.02–10 µg/mL [49-51].

Synthesis

SSA **1** was obtained through the addition of tetrabutylammonium (TBA) aminomethane sulphonate (AMS) to 1-adamantyl isocyanate and isolated as a yellow oil in a yield of 84%. SSA **3** was obtained through the reduction of intermediate **2**, to produce the corresponding amine, which was then reacted with triphosgene to give the corresponding isocyanate. This isocyanate was then reacted with TBA AMS to give **3**, which was obtained as a white solid in a yield of 62%.

Results and discussion

To enable the effective characterisation of SSA self-association events, an effective multi-component experimental approach has been developed (Figure 2) [20].

In the solution state, the self-associative properties of SSAs **1** and **3** were explored in DMSO-d_6/0.5% H_2O and $H_2O(D_2O)$/EtOH 19:1, to enable comparison with previously published SSA data [15,16]. Quantitative ^{1}H NMR (qNMR) studies allow, though comparative signal integration with an internal standard, for the percentage of a molecular component apparently 'lost' from solution to be calculated. Here, the presence of higher order self-association events causes those molecules involved in these processes to adopt solid-like properties, as larger aggregated species are produced, no longer detectable through traditional solution state ^{1}H NMR techniques.

Proton qNMR studies conducted in D_2O/EtOH 19:1, where EtOH acts as the internal standard, confirmed the presence of aggregated species of SSA **3** at 5.56 mM. Under these conditions, 50% of the SSA cationic and anionic components were found to be involved in the construction of these higher-order self-association events. Interestingly, these aggregated species also prevail in an organic solvent system; however, the percentage SSA **3** 'loss' is shown to decrease by approximately half. At a concentration of 112 mM in DMSO-d_6 standardised with 1% DCM, a ≈ 25% 'loss' of both SSA cationic and anionic components is observed. SSA **1** displayed no loss of either component in any of those same solvent systems; therefore, we find no evidence of higher-order SSA self-association events for this SSA at the concentrations tested within detectable limits. We hypothesise that self-association events of SSA **1** are hindered due to the positioning of the lipophilic adamantane moiety limiting access to the principal HBD urea group within the SSA molecular structure.

After undergoing an annealing process, the hydrodynamic diameter (d_H) of those self-associated aggregates produced by SSA **3** in a H_2O/EtOH 19:1 solution at 5.56 mM and DMSO at 112 mM were obtained via

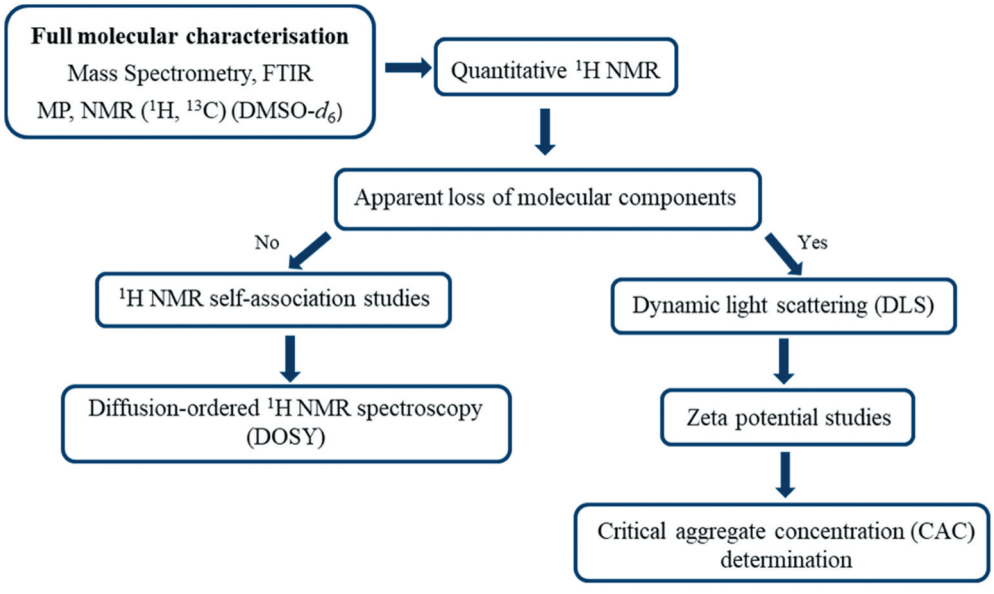

Figure 2. A schematic representation of the multi-component experimental approach to enable the characterisation of SSA self-association events.

dynamic light scattering (DLS) studies (Table 2). In a H_2O/EtOH 19:1 solution, the d_H of aggregates formed from SSA **3**, obtained from intensity distribution peak maxima, were found to be 127 nm, a value in line with results from previous studies [15,16,29]. Switching to a DMSO solvent system, the d_H was found to be seven times greater. Here, a value of 897 nm was obtained, likely to be due to the amalgamation of smaller aggregated units instead of that of singular units as observed in an H_2O/EtOH 19:1 solvent system.

(a) No 'loss' observed in [1]H qNMR studies; *b* – CAC above the limit of solubility.

Surface tension data derived from tensiometry measurements were used to calculate critical aggregate concentration (CAC) at 298 K. The CAC value for an SSA was determined as the point at which the surface tension of a solution no longer decreases with increasing compound concentration [52]. However, at concentrations below CAC, aggregates can still exist in solution [53], thus allowing for the observation of those larger self-associated aggregates at concentrations lower than the CAC. The CAC value for **1** in a H_2O/EtOH 19:1 solution was calculated to be 85.4 mM. At this concentration, the aggregates present were found to be relatively stable, exhibiting a zeta potential of −36 mV. Due to the limit of solubility, the CAC value for SSA **3** was recorded at 6 mM, at which the aggregates formed were shown to be comparatively unstable, exhibiting a zeta potential value of −8 mV.

To verify the presence of any low-level hydrogen-bonded self-association events involving **1** or **3**, ^{1}H NMR dilution and ^{1}H NMR DOSY (diffusion-ordered spectroscopy) studies were performed in a DMSO-d_6 /0.5% H_2O solvent system, in line with previous studies [15,16,54]. Calculated molecular length values for the anionic component of both SSA **1** and 3 were obtained using ChemBio3D after application of MM2 energy minimisation methods. The results showed the anionic component of SSAs **1** and **3** has a molecular length of 9.87 Å (0.99 nm) and 12.30 Å (1.23 nm), respectively. Comparatively, a ^{1}H NMR DOSY study performed with **1** confirmed the formation of only these lower order self-associated or monomeric species present in solution at 112 mM, with the anionic component of the SSA exhibiting a d_H of 1.41 nm. This is supported by the results obtained from our MM2 energy minimised computational modelling methods. The change in up field chemical shift of the urea HBD groups observed through ^{1}H NMR dilution studies was used to confirm the presence of hydrogen bonding self-association events, while fitting these data to self-associative binding isotherms (where possible) using BindFit v0.5 [55] enables the quantification of the strength of these same interactions. The data obtained from ^{1}H NMR dilution studies conducted with SSA **1** (Figure 3a) could not be fitted to either the *Cooperative Equal K* or *Equal K/ Dimerisation model* binding isotherms, which is unsurprising as the overall change in chemical shift observed for these HBD urea NH's is small, which, coupled with the linear nature of these trends, suggests the absence of significant SSA anion hydrogen bonding self-association events present under these experimental conditions. Again, this furthers supports our earlier hypothesis that this is due to the limited accessibility to the principle HBD site present within this SSA anion because of the steric hinderance provided by the adamantane functionality. Although the chemical shift data for SSA **3** could not be fitted to either the *Cooperative Equal K* or *Equal K/ Dimerisation model* binding isotherms due to the presence of higher-order aggregates species within the solution (Table 1), it was possible to verify that the phenyl amide NH was not involved in any low-level self-association events as depicted in Figure 3b. However, we do see evidence of the SSA anion association through the formation of urea-mediated hydrogen bonds through the downfield change in chemical shift for these NH resonances with increasing compound concentration.

We have previously shown that simple low-level computational modelling techniques can be utilised in the prediction of physicochemical properties of our library of SSAs [15,16,28]. Derived from low-level computational modelling using geometry optimised, semi-empirical PM6 molecular models, electrostatic surface potential maps were used to identify the location and quantify theoretical electrostatic potential surface maxima (E_{max}) and minima (E_{min}) values, in line with previous work from both Hunter and Stewart [56,57]. Using this combined methodology, the E_{max} and E_{min} values were calculated for optimised linear versions of the anionic component of SSAs **1** and **3**. The E_{max} and E_{min} values were found to correlate with the primary HBD and HBA functionalities within the molecular structure, supporting the findings of Hunter's original work (Figure 4) [56].

These data support our earlier hypothesis that for SSA **1**, inaccessibility of the urea NH's was a contributing factor towards a decreased prevalence of solution state SSA self-association events in comparison to SSA **3**. In addition, the E_{max} values obtained from these electrostatic potential maps that are hypothesised to correlate with principle HBD activity suggest the urea NH's of SSA **3** to be better optimised towards the formation of stronger self-associative hydrogen bonds than SSA **1**, exhibiting values of +23 KJ/mol and −101 KJ/mol, respectively.

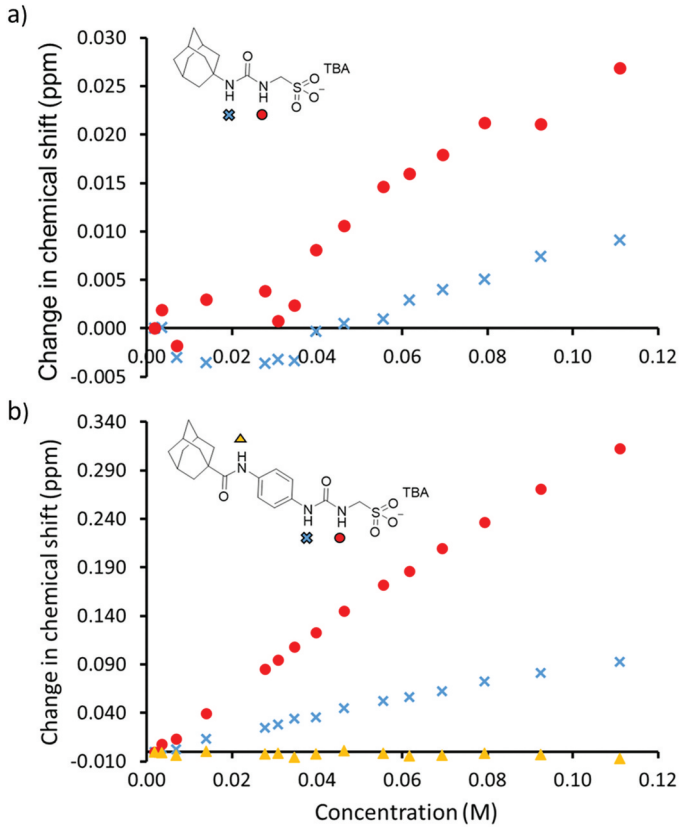

Figure 3. Graph summarising the ^{1}H NMR down-field change in chemical shift of urea and amide NH resonances with increasing concentration of (a) SSA **1** and (b) SSA **3** in DMSO-d_6 0.5% H_2O (298 K).

Table 1. Summary of quantitative ^{1}H NMR studies.

	Quantitative ^{1}H NMR			
	DMSO-d_6 (%)		D_2O (%)	
SSA	Anion	Cation	Anion	Cation
1	0	0	0	0
3	26	27	48	49

Values given in % represent the observed proportion of compound that has become NMR silent, and thus is apparently 'lost' from solution for 1 and 3. Studies performed at concentrations of ≈ 112 mM in DMSO-d6 standadised with 1% DCM and 5.56 mM in D2O standardised with 5% EtOH.

Table 2. Summary of physicochemical data produced to characterise SSA self-association events. DLS intensity particle size distribution peak maxima of **3** obtained at 5.56 mM in a solution of H_2O/EtOH 19:1 and at 111.2 mM in DMSO. Critical aggregate concentration (CAC) was derived at approximately 291 K from surface tension measurements [52].

	d_H (nm)			
SSA	DMSO	H_2O/EtOH 19:1	CAC (mM)	Surface tension at CAC (mN/m)
1	*a*	*a*	85.4	34.86
3	897	127	*b*	*b*

Antimicrobial activity and toxicity studies

We have previously shown that SSAs exhibit antimicrobial activity against clinically relevant strains of Gram-positive MRSA USA300 and Gram-negative *E. coli* DH10B [17,28,29]. Here, we add to those previously published data sets elucidating the activity of both SSA **1** and SSA **3** against these same model bacterial strains. To establish whether these SSAs are bactericidal or bacteriostatic, complete death must occur, which is beyond the limit of solubility for SSAs **1** and **3**. The results from these

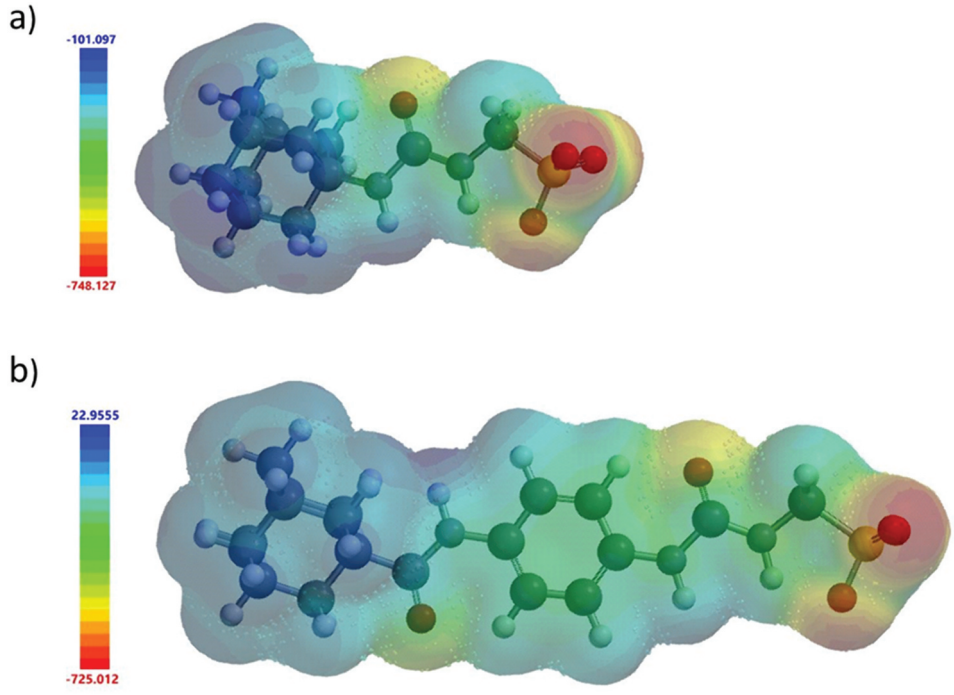

Figure 4. Electrostatic potential maps calculated for the anionic component of (a) SSA **1** and (b) SSA **3**. E_{max} and E_{min} values depicted in the figure legends are given in KJ/mol. Dots indicate inaccessible areas on the molecular surface.

MIC_{50} microbial efficacy studies are presented in Figure 5. At 5 mM, SSA **1** exhibited activity against both strains of bacteria resulting in a 46% inhibition of bacterial growth against MRSA and a 56% against *E. coli* (Figure 5a and c). Unlike SSA **1**, SSA **3** exhibits Gram-positive bacterial selectivity, resulting in an 86% inhibition of MRSA (Figure 5b) versus no inhibition of *E. coli* bacterial growth (Figure 5d).

Interestingly, through a simple structural modification – removal of the phenyl amide functionality present

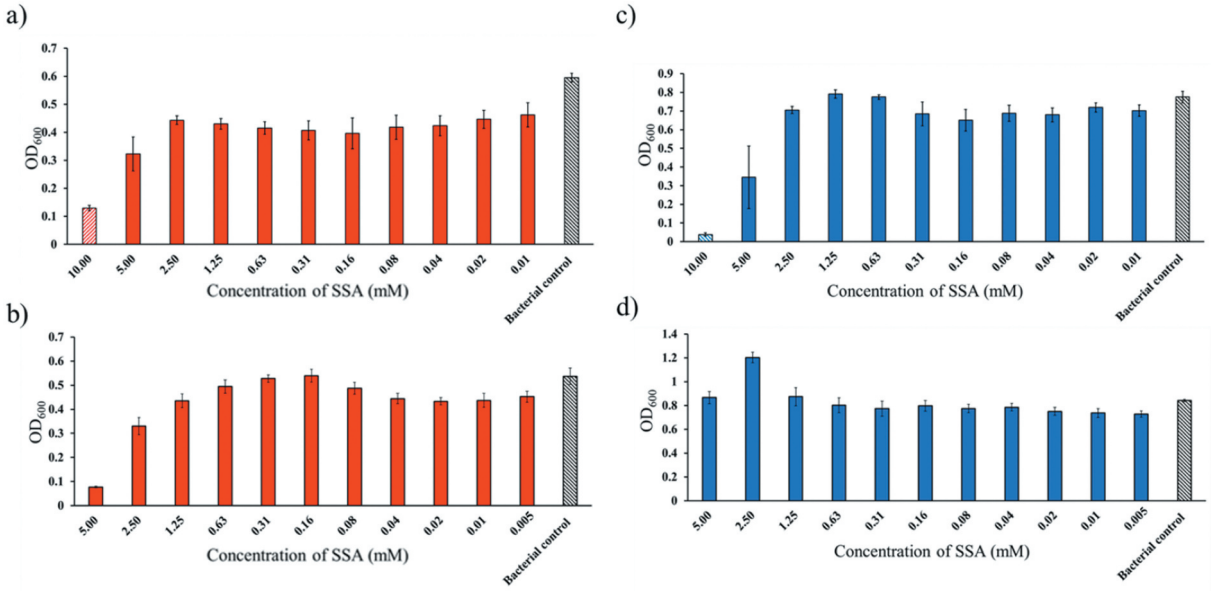

Figure 5. Average (n = 3) bacterial growth profiles of: MRSA USA300 incubated with 0 mM–10 mM of (a) SSA **1** and (b) SSA **3**; E. coli DH10B incubated with 0 mM–10 mM of (c) SSA **1** and (d) SSA **3**. Here, the SSAs were supplied to the bacterial culture as a EtOH/H_2O 1:19 solution; therefore, these experimental results are standardised against a control EtOH/H_2O 1:19 solution. OD_{600} measurements were taken at 900 min.

Table 3. Summary of % haemolysis results obtained for **1** and **3** at 1.39 mM and a H_2O/EtOH 19:1 control solution obtained in PBS buffer [58].

	% Haemolysis				
SSA	Repeat 1	Repeat 2	Repeat 3	AVG	SD
1	0.5	0.5	1.0	0.7	0.29
3	1.0	0.8	1.0	0.9	0.11
5% EtOH	0.5	0.6	0.5	0.5	0.05

Error = standard deviation to 2 dp. The haemolysis results were obtained at this concentration due to limited SSA solubility in PBS buffer.

in SSA **3**, to produce SSA **1** – we find SSA **1** maintains activity against Gram-negative *E. coli*, while SSA **3** becomes inactive towards this same bacteria. This is hypothesised to be due to the increase in lipophilicity of the anionic component of the SSA (as a result of amide and phenyl substituent removal), and perhaps deactivation of the urea NH functionality. These data provide evidence towards the hypothesis that it is possible to further develop SSA technology, tailoring the activity of an SSA towards specific target bacteria.

To explore the potential for this SSA technology to be developed towards the clinic, a preliminary toxicity profile was established for SSAs **1** and **3** against human erythrocytes (Table 3). Here, the SSA was added to the erythrocytes in a H_2O/EtOH 19:1 solution to ensure that the SSA haemolysis effects can be related to those SSA aggregates discussed previously and present within the antimicrobial activity studies.

The average percentage haemolysis of human erythrocytes in the presence of SSAs **1** and **3** (1.39 mM) was found to be <1.0%. Furthermore, the concentration of SSAs **1** and **3** required to lyse 10% of those erythrocytes present was found to be >5 mM in both instances, showing that these SSAs demonstrate a greater activity towards bacterial cells (specifically MRSA) over human erythrocytes at this concentration.

To establish the toxicity of SSAs **1** and **3** towards multicellular organisms, *Galleria mellonella* larvae were injected with 10 µL of SSA (5 mM) in a dH_2O/EtOH 19:1 solution and then incubated at 37°C for a maximum of 5 days. Each day, the number of surviving larvae were counted (Table 4). The results of these studies showed SSA **3** to be far more toxic than SSA **1**. This demonstrates a clear structure activity relationship; the presence of the amide appended phenyl ring system within the anionic component of SSA **3** dramatically increases the toxicity of this compound towards this multicellular organism. In addition, the maintenance of larvae survival rates (days 2–5) provides some evidence that SSA **3** maybe acutely toxic, since, after an initial 60% death rate over 24 hours, the rest of the larvae survived the 5-day experiment.

Conclusion

We have synthesised two novel, next-generation adamantane incorporated SSAs, **1** and **3** (Figure 1). The self-associative properties of these SSAs in both a DMSO-d_6 /0.5% H_2O and $H_2O(D_2O)$/EtOH 19:1 were explored. The presence of the amide substituted phenyl ring system within the structure of SSA **3** results in the production of higher-order aggregated species within both solvent systems at lower concentrations than was observed with SSA **1**. This is thought to be due to a combination of decreased accessibility to the principle HBD group of **1**, and comparative deactivation of this same functionality towards the formation of self-associative hydrogen bonds. This hypothesis is supported by the results of complimentary low-level computational modelling and ^{1}H NMR dilution studies.

Furthermore, we report the antimicrobial efficacy of **1** and **3** against clinically relevant Gram-positive MRSA and Gram-negative *E. coli*, and show that SSA **1** demonstrates limited activity against both model bacteria, which, we hypothesise, is due to the removal of the amide appended phenyl ring system, increasing the general lipophilic properties of the SSA anionic component. Finally, we confirm both **1** and **3** to demonstrate limited toxicity towards erythrocytes; however, when injected into *G. mellonella* larvae, SSA **3** was

Table 4. Results from the Galleria mellonella toxicity studies for **1** and **3** (5 mM, 10 µL), phosphate-buffered saline (PBS) and 5% EtOH, over a 5-day period.

	Quantity of *Galleria mellonella* larvae alive days 0–5					
SSA	0	1	2	3	4	5
1	10	9	9	9	9	9
3	10	4	4	4	4	4
PBS	10	10	10	10	10	10
5% EtOH	10	10	10	10	10	10

found to demonstrate considerably higher levels of toxicity towards this multicellular organism over SSA **1**.

Acknowledgments

A. Rutkauskaite, L.White, J.Boles, K. Hilton and J. Hiscock would like to thank the University of Kent for funding. Additionally, J. Hiscock and L. White would also like to thank UKRI for the funding of J. Hiscock's Future Leaders Fellowship (MR/T020415/1). J. Boles thank UKHSA for the funding of her PhD studentship.

Disclosure statement

No potential conflict of interest was reported by the authors.

Funding

This work was supported by the UKHSA [PhD studentship funding]; UK Research and Innovation [MR/T020415/1].

Notes on contributors

Dr. Lisa White is a first-generation higher educated woman, who returned to education at the University of Kent as a mature student in her late 30's. At this time she had four children at home two of which were under the age of four. In 2016 she obtained her bachelor's degree with hons. in Forensic science. Following this she chose to continue her academic pathway, going on to study for an MRes in chemistry under the supervision of Prof. Jennifer Hiscock. During her MRes, Lisa became a grandmother for the first time, and three years later her second grandson made his appearance, due to family commitments and the vicinity of the campus to her home the University of Kent was ideally situated. Lisa then remained with Prof. Hiscock for a further three years whilst working towards her PhD, subsequently followed by a PDRA position, where her work explores the potential for supramolecular self-associating amphiphiles for use as antimicrobial agents.

Melanie Clifford is a first-generation higher educated woman, who returned to education as a mature student at the age of 34. At this time, she also worked full time for the UK Health Security Agency (UKHSA) as a research scientist, firstly evaluating tAK as a decontamination analysis tool then, secondly evaluating novel antimicrobial compounds. In 2018 she obtained her bachelor's degree with hons in Natural Sciences from the Open University. Since completing her degree she continued to work for UKHSA researching novel antimicrobial compounds and their effectiveness against antimicrobial resistant pathogens. She has recently moved on to Defence Science and Technology Laboratories as a workplace manager for the Cyber and Information Systems Division.

Bree Streather is the first in her family to have entered into higher education. After her A levels in 2017, she began her studies at the University of Kent, and was awarded a 1st class Bachelor's degree in Biochemistry. She went on to complete a Master's by research at the University under the supervision of Dr Chris Mulligan, where she investigated the structure of a membrane transporter thought to be involved in antimicrobial resistance. During this period, she discovered an inner passion for biological laboratory research, and subsequently applied and was accepted onto the BBSRC funded SocoBio Doctoral Training Programme, where she has the opportunity to work in labs across 4 universities, and will undertake a period working in industry. She is now in the second year of this 4-year PhD programme, working with Professors Mulvihill and Hiscock on a multidisciplinary project examining the mode of action of novel Supramolecular Self-associating (SSA) antimicrobials.

Professor Dan Mulvihill is a first-generation higher educated adult, who returned to higher education in his 20's to undertake a B.Sc. in Genetics at the University of London, and subsequent PhD in Cell Biology at the Universities of Dundee and Manchester. His passion for biological research led him to postdoctoral research positions at the University College London and Hannover Medical School. Based upon the success of his research, he was subsequently awarded a 5-year BBSRC David Phillips Research Fellowship, which provided him with the opportunity to return to the UK to set up an independent research group at the University of Kent, to study the role of molecular motors in regulating the growth and cell division. His research group has flourished in the supportive and collegiate environment within the Kent School of Biosciences ever since. Having stepped down from roles of Associate Dean for Research for Sciences, and the Head of Biosciences, he is currently the Professor of Cell and Molecular Biology.

ORCID

Daniel P. Mulvihill http://orcid.org/0000-0003-2502-5274
Mark Shepherd http://orcid.org/0000-0002-7472-2300
Jennifer R. Hiscock http://orcid.org/0000-0002-1406-8802

References

[1] Murray CJ, Ikuta KS, Sharara F, et al. Antimicrobial Resistance Collaborators. Global burden of bacterial antimicrobial resistance in 2019: a systematic analysis. Lancet. 2022;399: 629–655.
[2] Davies S, Farrar J, Rex J, et al. Antimicrobial resistance: tackling a crisis for the health and wealth of nations. HM Government and Wellcome Trust. 2014; 1–20.
[3] Drug-Resistant Infections, World Bank. Washington DC. 2017 https://www.worldbank.org/en/topic/health/publication/drug-resistant-infections-a-threat-to-our-economic-future.
[4] Bright-Ponte SJ. Antimicrobial use data collection in animal agriculture. Zoonoses Public Health. 2020;67(S1):1–5.
[5] Davey P, Marwick CA, Scott CL, et al. Interventions to improve antibiotic prescribing practices for hospital inpatients. Cochrane Database Syst Rev. 2017;2:1–315.
[6] Kazanjian PH. Efforts to regulate antibiotic misuse in hospitals: a history. Infect Control Hosp Epidemiol. 2022;43(9):1119–1122.
[7] Pechère JC. Patients' interviews and misuse of antibiotics. Clin Infect Dis. 2001;33(s3):S170–S173.

[8] Knight GM, Glover RE, McQuaid CF, et al. Antimicrobial resistance and COVID-19: intersections and implications. Elife. 2021;10:e64139.
[9] Lai -C-C, Chen S-Y, Ko W-C, et al. Increased antimicrobial resistance during the COVID-19 pandemic. Int J Antimicrob Agents. 2021;57(4):106324.
[10] Founou RC, Blocker AJ, Noubom M, et al. The COVID-19 pandemic: a threat to antimicrobial resistance containment. Futur Sci OA. 2021;7:8.
[11] Ruiz J. Enhanced antibiotic resistance as a collateral COVID-19 pandemic effect? J Hosp Infect. 2021;107:114–115.
[12] Zhou M, Zheng M, Cai J. Small molecules with membrane-active antibacterial activity. ACS Appl Mater Interfaces. 2020;12(19):21292–21299.
[13] Dey R, De K, Mukherjee R, et al. Small antibacterial molecules highly active against drug-resistant Staphylococcus aureus. Medchemcomm. 2019;10 (11):1907–1915.
[14] Hamad M, Al-Marzooq F, Srinivasulu V, et al. Small antibacterial molecules highly active against drug-resistant Staphylococcus aureus. Front Microbiol. 2022;13:1–14.
[15] White LJ, Wells NJ, Blackholly LR, et al. Towards quantifying the role of hydrogen bonding within amphiphile self-association and resultant aggregate formation. Chem Sci. 2017;8(11):7620–7630.
[16] White LJ, Tyuleva SN, Wilson B, et al. Towards the prediction of global solution state properties for hydrogen bonded, self-associating amphiphiles. Chem Eur J. 2018;24(30):7761–7773.
[17] White LJ, Boles JE, Clifford M, et al. Di-anionic self-associating supramolecular amphiphiles (SSAs) as antimicrobial agents against MRSA and *Escherichia coli*. Chem Commun. 2021;57(89):11839–11842.
[18] Ng KKL, Dimitrovski M, Boles JE, et al. Towards the use of (pseudo) nucleobase substituted amphiphiles as DNA nucleotide mimics and antimicrobial agents. Supramol Chem. 2020;32(7):414–424.
[19] White LJ, Boles JE, Allen N, et al. Controllable hydrogen bonded self-association for the formation of multifunctional antimicrobial materials. J Mater Chem B. 2020;8 (21):4694–4700.
[20] White LJ, Boles JE, Hilton KLF, et al. Towards the application of supramolecular self-associating amphiphiles as next-generation delivery vehicles. Molecules. 2020;25 (18):4126.
[21] Gumbs TL, White LJ, Wells NJ, et al. 'Frustrated' hydrogen-bonded self-associated systems as templates towards DNA incorporated nanostructure formation. Supramol Chem. 2018;30(4):42–51.
[22] Blackholly LR, Shepherd HJ, Hiscock JR. 'Frustrated' hydrogen bond mediated amphiphile self-assembly – a solid state study. CrystEngComm. 2016;18 (37):7021–7028.
[23] Townshend G, Thompson GS, White LJ, et al. The elucidation of phospholipid bilayer–small molecule interactions using a combination of phospholipid nanodiscs and solution state NMR techniques. Chem Commun. 2020;56(28):4015–4018.
[24] Medina-Carmona E, Varela L, Hendry AC, et al. A quantitative assay to study the lipid selectivity of membrane-associated systems using solution NMR. Chem Commun. 2020;56(78):11665–11668.
[25] Dora NO, Blackburn E, Boles JE, et al. Supramolecular self-associating amphiphiles (SSAs) as nanoscale enhancers of cisplatin anticancer activity. RSC Adv. 2021;11 (23):14213–14217.
[26] Boles JE, Williams GT, Allen N, et al. Anionic Self-Assembling Supramolecular Enhancers of Antimicrobial Efficacy against Gram-Negative Bacteria. Adv Ther. 2022;5:1–9.
[27] Boles JE, Ellaby RJ, Shepherd HJ, et al. Supramolecular self-associating amphiphiles (SSAs) as enhancers of antimicrobial agents towards *Escherichia coli* (E. coli). RSC Adv. 2021;11(16):9550–9556.
[28] Allen N, White LJ, Boles JE, et al. Towards the prediction of antimicrobial efficacy for hydrogen bonded, self-associating amphiphiles. ChemMedChem. 2020;15 (22):2193–2205.
[29] Tyuleva SN, Allen N, White LJ, et al. A symbiotic supramolecular approach to the design of novel amphiphiles with antibacterial properties against MSRA. Chem Commun. 2019;55(1):95–98.
[30] Wanka L, Iqbal K, Schreiner PR. The lipophilic bullet hits the targets: medicinal chemistry of adamantane derivatives. Chem Rev. 2013;113(5):3516–3604.
[31] Štimac A, Šekutor M, Mlinarić-Majerski K, et al. Adamantane in drug delivery systems and surface recognition. Molecules. 2017;22(2):297.
[32] Dong G, Peng C, Luo J, et al. Adamantane-Resistant Influenza A Viruses in the World (1902–2013): Frequency and Distribution of M2 Gene Mutations. PLoS One. 2015;10:1–20.
[33] Vernier VG, Harmon JB, Stump JM, et al. The toxicologic and pharmacologic properties of amantadine hydrochloride. Toxicol Appl Pharmacol. 1969;15 (3):642–665.
[34] Kolocouris N, Foscolos GB, Kolocouris A, et al. Synthesis and antiviral activity evaluation of some aminoadamantane derivatives. J Med Chem. 1994;37(18):2896–2902.
[35] Bright RA, Medina M, Xu X, et al. Incidence of adamantane resistance among influenza A (H3N2) viruses isolated worldwide from 1994 to 2005: a cause for concern. Lancet. 2005;366(9492):1175–1181.
[36] El-Emam AA, Al-Deeb OA, Al-Omar M, et al. Synthesis, antimicrobial, and anti-HIV-1 activity of certain 5-(1-adamantyl)-2-substituted thio-1,3,4-oxadiazoles and 5-(1-adamantyl)-3-substituted aminomethyl-1,3,4-oxadiazoline-2-thiones. Bioorg Med Chem. 2004;12(19):5107–5113.
[37] Printsevskaya SS, Solovieva SE, Olsufyeva EN, et al. Structure–activity relationship studies of a series of antiviral and antibacterial aglycon derivatives of the glycopeptide antibiotics vancomycin, eremomycin, and dechloroeremomycin. J Med Chem. 2005;48(11):3 885–3890.
[38] Burstein ME, Serbin AV, Khakhulina TV, et al. Inhibition of HIV-1 replication by newly developed adamantane-containing polyanionic agents. Antiviral Res. 1999;41 (3):135–144.
[39] Balzarini J, Orzeszko B, Maurin JK, et al. Synthesis and anti-HIV studies of 2-adamantyl-substituted thiazolidin-4-ones. Eur J Med Chem. 2007;42(7):993–1003.

[40] Tillmann HL. Hepatitis C virus infection and the brain. Metab Brain Dis. 2004;19(3/4):351–356.
[41] Singh C, Kanchan R, Sharma U, et al. New adamantane-based spiro 1,2,4-trioxanes orally effective against rodent and simian malaria. J Med Chem. 2007;50 (3):521–527.
[42] Wang X, Dong Y, Wittlin S, et al. Spiro- and dispiro-1,2-dioxolanes: contribution of iron(II)-mediated one-electron vs two-electron reduction to the activity of antimalarial peroxides. J Med Chem. 2007;50 (23):5840–5847.
[43] Kouatly O, Geronikaki A, Kamoutsis C, et al. Adamantane derivatives of thiazolyl-N-substituted amide, as possible non-steroidal anti-inflammatory agents. Eur J Med Chem. 2009;44(3):1198–1204.
[44] Kadi AA, El-Brollosy NR, Al-Deeb OA, et al. Synthesis, antimicrobial, and anti-inflammatory activities of novel 2-(1-adamantyl)-5-substituted-1,3,4-oxadiazoles and 2-(1-adamantylamino)-5-substituted-1,3,4-thiadiazoles. Eur J Med Chem. 2007;42(2):235–242.
[45] Shen C, Bullens D, Kasran A, et al. Inhibition of glycolipid biosynthesis by N-(5-adamantane-1-yl-methoxy-pentyl)-deoxynojirimycin protects against the inflammatory response in hapten-induced colitis. Int Immunopharmacol. 2004;4(7):939–951.
[46] Bai H, Yuan H, Nie C, et al. A supramolecular antibiotic switch for antibacterial regulation. Angew Chem Int Educ. 2015;54(45):13208–13213.
[47] Yang Y, Cai Z, Huang Z, et al. Antimicrobial cationic polymers: from structural design to functional control. Polym J. 2018;50(1):33–44.
[48] Orzeszko A, Kamińska B, Starościak BJ. Synthesis and antimicrobial activity of new adamantane derivatives III. Farm. 2002;57(8):619–624.
[49] Orzeszko A, Kamińska B, Orzeszko G, et al. Synthesis and antimicrobial activity of new adamantane derivatives II. Farmaco. 2000;55(9–10):619–623.
[50] White LJ, Boles JE, Hilton KLF, et al. Towards the application of supramolecular self-associating amphiphiles as next-generation delivery vehicles. Molecules. 2020;25 (18):4126.
[51] White LJ, Tyuleva SN, Wilson B, et al. Towards the prediction of global solution state properties for hydrogen bonded, self-associating amphiphiles. Chem Eur J. 2018;24(30):7761–7773.
[52] Piñeiro Á, Banquy X, Pérez-Casas S, et al. On the characterization of host–guest complexes: surface tension, calorimetry, and molecular dynamics of cyclodextrins with a non-ionic surfactant. J Phys Chem B. 2007;111(17):4383–4392.
[53] Nagarajan R, Ruckenstein E. Theory of surfactant self-assembly: a predictive molecular thermodynamic approach. Langmuir. 1991;7(12):2934–2969.
[54] Hiscock JR, Bustone GP, Wilson B, et al. In situ modification of nanostructure configuration through the manipulation of hydrogen bonded amphiphile self-association. Soft Matter. 2016;12:4221–4228.
[55] Supramolecular.org - Binding Constant Calculators | Supramolecular, http://app.supramolecular.org/bindfit/, (accessed 2020 Jul 1).
[56] Hunter CA. Quantifying intermolecular interactions: guidelines for the molecular recognition toolbox. Angew Chem Int Educ. 2004;43(40):5310–5324.
[57] Stewart JJP. Optimization of parameters for semiempirical methods V: modification of NDDO approximations and application to 70 elements. J Mol Model. 2007;13 (12):1173–1213.
[58] Travis SM, Anderson NN, Forsyth WR, et al. Bactericidal activity of mammalian cathelicidin-derived peptides. Infect Immun. 2000;68(5):2748.